Characterization of the Preparation of Pd/SiO$_2$ and Pd/La$_2$O$_3$ by Laser Raman Spectroscopy

SHIRLEY S. CHAN* AND ALEXIS T. BELL†

*Exxon Research and Engineering Company, Route 22 East, Annandale, New Jersey 08801, and †Materials and Molecular Research Division, Lawrence Berkeley Laboratory, and Department of Chemical Engineering, University of California, Berkeley, California 94720

Multichannel laser Raman spectroscopy has been used to characterize the chemistry occurring during the preparation of silica and lanthanum oxide supported palladium catalysts from PdCl$_2$. The results show that the structure of lanthanum oxide is a strong function of its state of hydration and evidence is reported for structures bridging the extremes of La(OH)$_3$ and La$_2$O$_3$. PdCl$_2$, used as the source of Pd, undergoes a change in crystal structure and then conversion to PdO when heated in air up to 773 K. Silica supported PdCl$_2$ undergoes a similar set of transformations. The spectrum of the lanthanum oxide-supported PdCl$_2$ is quite different from that supported on silica, but the exact structure of the supported species cannot be determined. Calcination produces a new species which is believed to be a mixed metal oxide of La and Pd.

INTRODUCTION

Several recent studies (*1–4*) have shown that palladium supported on lanthanum oxide, or silica promoted with lanthanum oxide, is an active and highly selective catalyst for the synthesis of methanol. The beneficial influence of the rare earth oxide has been attributed to the existence of a metal–support interaction. Characterization of a set of Pd/La$_2$O$_3$ catalysts by XPS (*5*) has shown that the Pd 3d$_{5/2}$ binding energy of the reduced catalysts lies as much as 0.7 eV below that of metallic Pd. By contrast, the binding energy of Pd supported on SiO$_2$ at an equivalent dispersion is virtually the same as for the bulk metal. The downscale shift in binding energy for Pd supported on La$_2$O$_3$ was attributed to the interaction of Pd atoms at the surface of the Pd crystallites with thin patches of LaO partially covering the crystallite surface. It was proposed that the patches of LaO are formed by partial reduction of patches of La$_2$O$_3$ [or possibly La(OH)$_3$] as a consequence of their intimate contact with the metal. Since the magnitude of the binding energy shift was observed to increase with decreasing dispersion, it was proposed that the coverage of the Pd crystallites by LaO patches increased with decreasing dispersion. This picture of La$_2$O$_3$-supported Pd has been supported recently by CO chemisorption studies. Hicks *et al.* (*6*) observed that the CO adsorption capacity of Pd/La$_2$O$_3$ is significantly less than that of Pd/SiO$_2$, and decreases as the dispersion decreases. It was also noted that the CO which does adsorb on Pd/La$_2$O$_3$ is more weakly bound than CO adsorbed on Pd/SiO$_2$. Both observations were attributed to a partial blockage of the Pd crystallite surfaces by patches of LaO.

The present paper reports on the use of multichannel laser Raman spectroscopy to characterize the preparation of La$_2$O$_3$-supported Pd. The results of observations concerning SiO$_2$-supported Pd are also presented for the purpose of comparison. The information obtained from Raman spectroscopy complements that obtained from XPS and contributes to establishing a more detailed understanding of catalyst composition.
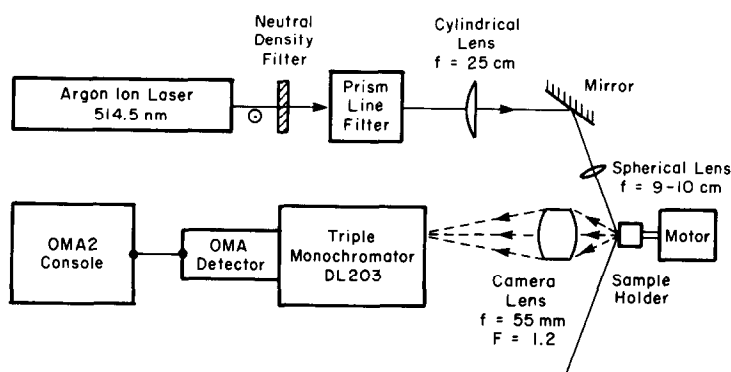
433

FIG. 1. Schematic diagram of the optical setup of the multichannel Raman spectrometer.

EXPERIMENTAL

Sample preparation. The two supports used in this study were Cab-O-Sil HS-5 silica (BET surface area 300 m²/g) and Union Molycorp. lanthanum oxide (BET surface area, ~11 m²/g). The lanthanum oxide was converted to lanthanum trihydroxide by refluxing in boiling water overnight. Palladium dichloride obtained from Ventron was converted to H_2PdCl_4 by dissolution in concentrated HCl followed by evaporation to dryness (7). To prepare the Pd/SiO_2 sample, H_2PdCl_4 was dissolved in 1 N HCl, and a small amount of the solution was contacted with the SiO_2. The water and excess HCl were removed by first drying the sample in air and then in a vacuum oven at 338 K. The Pd/La_2O_3 sample was prepared by dropwise addition of a H_2PdCl_4 solution to a slurry of $La(OH)_3$. Following this step, the slurry was heated to 338 K for 12 hr and then filtered. The filtrate was thoroughly washed with water and dried in a vacuum oven at 338 K. Portions of the supported precursor were calcined in a O_2/He mixture at 623 K for 2 hr and then reduced in pure H_2 at 573 K for 3 hr. The Pd weight loading of the reduced samples, determined by X-ray fluorescence and quantitative analysis, are 9.0% for Pd/SiO_2 and 5.0% for Pd/La_2O_3. The Pd dispersions, determined by H_2-O_2 titration (6), are 18% for Pd/SiO_2 and 9% for Pd/La_2O_3. The samples used in the

Raman studies were also characterized by X-ray diffraction (XRD).

Apparatus. Figure 1 shows the schematic diagram of the optical setup of the multichannel laser Raman spectrometer at Exxon. An Argon ion laser (Spectra Physics, Model 165) tuned to the 514.5 nm line was used for excitation. A prism monochromator (Anaspec Model 300S) which has a typical band width of 0.3 nm was used to remove the laser plasma lines. A cylindrical lens ($f = 250$ mm) and a variable spherical lens ($f = 90-100$ mm) were used to achieve an elliptically focused image on the sample. Each sample of about 0.2 g was pelletized under 5–10 kpsi pressure into a 16-mm-diameter wafer for mounting on a sample holder capable of spinning and *in situ* treatment. The laser power at the sample location was set in the range 0.4–160 mW by adding or removing neutral density filters.

The scattered light was collected by a camera lens (F/1.2, f/55 mm) held at about 45° with respect to the excitation. The Raman spectrometer was a triple monochromator (Instruments S.A., Model DL 203) equipped with holographic gratings and F4 optics. The spectrometer was coupled to an optical multichannel analyzer (Princeton Applied Research, Model OMA2) equipped with an intensified photodiode array detector cooled to $-15°C$. This optical multichannel analyzer system could deliver a spectrum about a factor of 100 faster than a
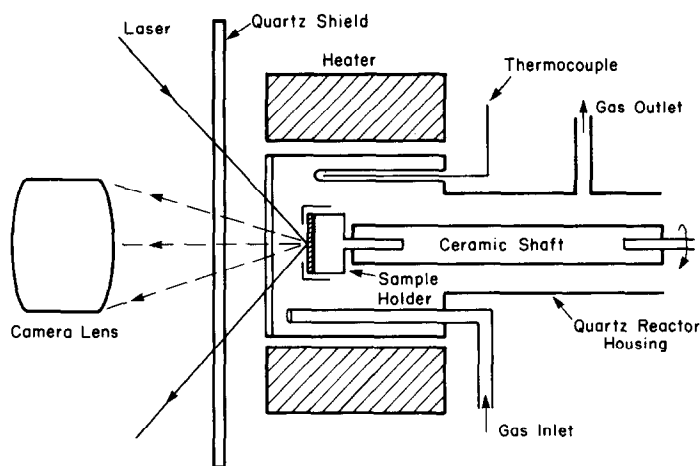
FIG. 2. Schematic diagram of the sample chamber.

conventional scanning spectrometer, and its averaging capability permitted measurements on samples of weak signals. The total accumulation time needed for each spectrum reported here typically was about 3 to 10 min. The digital display of the spectrum was calibrated to give 1.7 cm^{-1}/channel, whereas the overall spectral resolution was about 6 cm^{-1}.

Figure 2 shows the schematic diagram of the sample chamber at Exxon. The sample holder was made out of a corrosion resistant alloy, Hastelloy C. The catalyst disc was held beneath a collar which in turn was screwed onto the holder. The holder was then mounted on a shaft made of an inert machinable ceramic, Mycor (Corning). This served as a thermal insulator and a coupler to a rotable shaft with a ferrofluidic high vacuum seal, driven by an air motor. The body of the sample chamber was a quartz cylinder with a water-cooled taper joint on one end and a quartz optical window on the other enlarged end. Gas mixtures used for oxidation or reduction of the sample were delivered from a manifold into the front end of the chamber and exited at the rear. The flow rate was set at 50–500 cm^3/min and the deliver pressure was 20–30 kPa. The temperature was measured by a thermocouple (type K) inserted in a sealed capillary temperature-well internal to the quartz chamber. The temperature gradient between the thermal couple and the sample was calibrated to be 25 ± 5 K when the operating temperature was set between 448 and 873 K. A cylindrical heater coil with a negative feedback control surrounded the quartz chamber.

RESULTS AND DISCUSSION

Prior to studying the supported Pd precursor, Raman spectra were taken of the pure support materials. No features were observed in the spectrum of silica over the region of 50 to 1200 cm^{-1}. The spectrum of lanthanum oxide exhibited a number of bands, the position and intensity of which depended on the degree of hydration of the support. Spectrum a in Fig. 3 was for La$_2$O$_3$ as received. Three sharp bands were observed at 105, 192, and 409 cm^{-1}. The frequencies of these bands are in excellent agreement with those reported for crystalline La$_2$O$_3$ [107, 195 and 410 cm^{-1}] (8–10). Following complete hydration of La$_2$O$_3$ by refluxing in boiling water, spectrum b in Fig. 3 was obtained. Six bands were observed at 140, 234, 284, 342, 452, and 600. The positions of these bands correspond very closely with those reported for crystalline La(OH)$_3$ [140, 227, 283, 342, 450, and
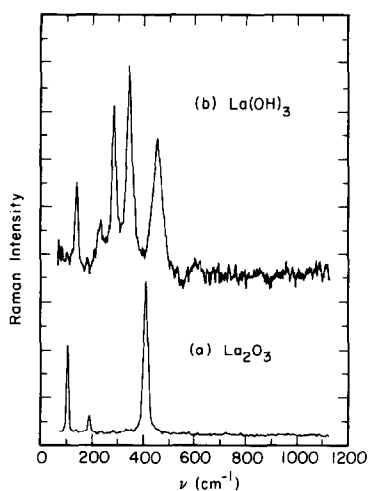
FIG. 3. Raman spectra of (a) La_2O_3 and (b) $La(OH)_3$.

603 cm^{-1}] (11). Furthermore, the XRD pattern of this hydrated La_2O_3 sample agreed completely with the pattern of $La(OH)_3$.

In situ calcination of $La(OH)_3$ in dry air produced a series of changes in the Raman spectrum as the temperature was raised (Fig. 4). Spectrum 4a was taken after heating the sample to 573 K and maintaining it there for 35 min. The bands seen in this spectrum were virtually the same as those observed for $La(OH)_3$ at room temperature (see spectrum 3b). When the temperature was increased to 623 K and held there for 30 min, the spectrum changed so that bands now appeared at 122, 133, 200, 227, 278, 306, 339, 378, and 423 cm^{-1} (spectrum 4b). Increasing the temperature to 673 K resulted in little additional change. The bands in spectrum 4c occurred at 122, 131, 191, 216, 306, 340, 378, and 421 cm^{-1} and were more intense than those seen in spectrum 4b. The final change in the spectrum was observed when the sample was heated to 773 K for 2.5 hr and cooled back to room temperature in ambient air. Spectrum 4d shows that in this case well defined features appeared at 105, 190, 316, and 407 cm^{-1} and weaker features were seen at 117, 381, 582, and 1066 cm^{-1}.

The spectra presented in Fig. 4 can be interpreted on the basis of what is known about the thermal decomposition of $La(OH)_3$. Studies by a number of authors (12-18) indicate that $La(OH)_3$ undergoes dehydration in a stepwise fashion as shown below.

$$La(OH)_3 \xrightarrow{623-675 \text{ K}} [La(OH)_2]_2O \xrightarrow{693-738 \text{ K}} LaO(OH) \xrightarrow{843-923 \text{ K}} La_2O_3$$
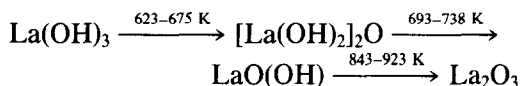
Consistent with this pattern, spectrum 4a shows that the sample remains as $La(OH)_3$ at 573 K. The change in the spectrum observed when the temperature is raised to 623 K (spectrum 4b) is very likely due to the conversion of $La(OH)_3$ to $[La(OH)_2]_2O$. This process is presumably accelerated when the temperature is increased to 723 K (see spectrum 4c). Spectrum 4d obtained after heating the sample to 773 K, shows clear evidence for La_2O_3 as indicated by the bands at 105, 190, and 407 cm^{-1}. The sharp band at 316 cm^{-1}, and possibly also those at 381 and 582 cm^{-1}, can be attributed to $LaO(OH)$.

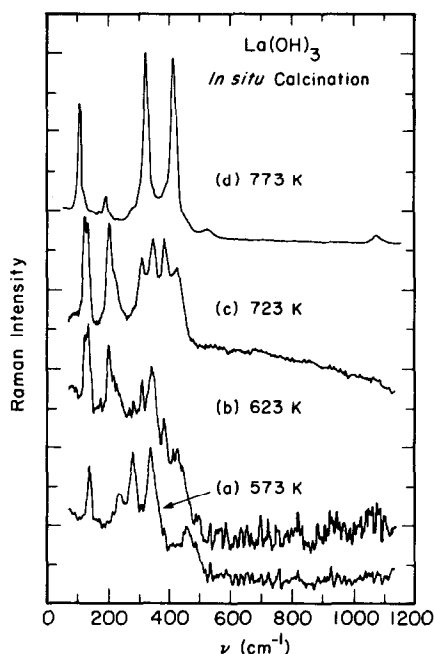
FIG. 4. *In situ* Raman spectra recorded during the dehydration of $La(OH)_3$ in dry air at various temperatures: (a) 573 K, 35 min; (b) 623 K, 30 min; (c) 723 K, 25 min; (d) 773 K, 150 min.
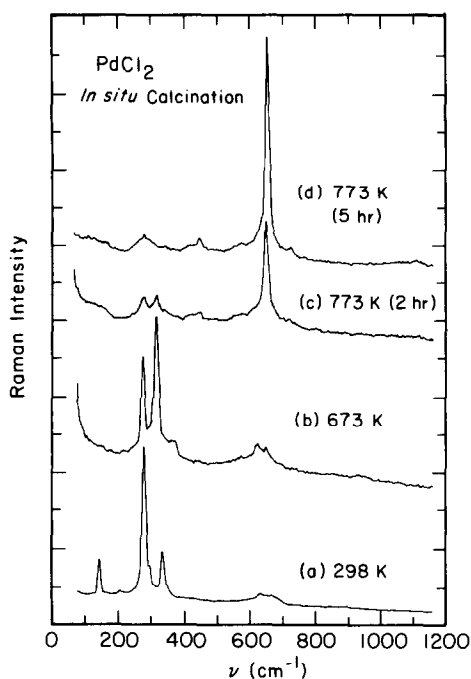
FIG. 5. *In situ* Raman spectra recorded during calcination of unsupported PdCl₂ in dry air at various temperatures: (a) 298 K; (b) 673 K, 2 hr; (c) 773 K, 2 hr; (d) 773 K, 5 hr.

The proposed interpretation of the spectra in Fig. 4 agrees very nicely with the XPS observations reported by Fleisch *et al.* (5). The O/La ratio determined from the XPS spectrum of La(OH)₃ calcined in air at 623 K was found to be 2.3, in rough agreement with what is expected for [La(OH)₂]₂O. Heating the sample in N₂ to 873 K reduced the O/La ratio to 1.5—the value expected for La₂O₃. It was also noted that as dehydration of the sample progressed, the La 3d₅/₂ binding energy shifted from 834.7 to 833.9 eV and the sattelite split increased from 3.7 to 4.0 eV. Both of these changes are characteristic of a conversion of La(OH)₃ to La₂O₃ (5, 19, 20).

The band at 1066 cm⁻¹ appearing in spectrum 4d can be assigned to lanthanum carbonate (21–25). The presence of carbonate groups was further confirmed by the observation of bands at 1400 and 1450 cm⁻¹ in the infrared spectrum of the calcined support. The XPS spectrum of the sample exhibited

a C1s peak at 288.8 eV, providing yet a further indicator of carbonate anions (5).

Figure 5 shows a series of spectra taken prior to, and during, the calcination of unsupported PdCl₂. Spectrum 5a, recorded at room temperature in dry air, exhibited bands at 147, 206, 278, 295, 335, 630, and 695 cm⁻¹. No significant change in the spectrum occurred until the temperature was raised to 673 K (spectrum 5b). At that point the bands at 147 and 335 diminished in intensity and a sharp, intense band appeared at 313 cm⁻¹. The two bands between 600 and 650 cm⁻¹ also increased in intensity. Raising the temperature to 773 K (spectrum 5c) resulted in a strong attenuation of the bands at 313 and 274 and the appearance of a sharp band at 650 cm⁻¹. This latter feature grew in intensity with prolonged heating at 773 K (spectrum 5d) and became the dominant feature in the spectrum.

The bands seen in Fig. 5 are difficult to assign since there have been relatively few Raman spectra published for compounds derivative from PdCl₂, and none for PdCl₂ itself. The features occurring below 380 cm⁻¹ are best assigned to stretching and bending vibrations in PdCl₂ on the basis of comparisons with the vibrational spectra reported for $PdCl_4^{2-}$, $PdCl_6^{2-}$, $Pd^{II}(NH_3)_2Cl_2$, $Pd^{IV}(NH_3)_2Cl_2$, $Pd^{II}Pd^{IV}(NH_3)_4Cl_4$, and Pd Cl₂ : Al₂Cl₆ (26–31) (see Table 1). The intense band at 648 cm⁻¹ plus the satellite bands at 573 and 722 cm⁻¹ observed in spectra 5c and 5d are due to PdO. Indeed the XRD of this sample confirmed that PdCl₂ had been converted to PdO. The weak bands appearing between 620 and 670 cm⁻¹ in spectra 5a and 5b are thus attributable to this same species. Since it is expected that the calcination of PdCl₂ will proceed through an oxychloride, it is likely that the weak bands observed at 414 and 445 cm⁻¹ are due to compounds with stoichiometries such as $PdO_{x/2}Cl_{2-x}$. The band at 276 cm⁻¹ is due to residual PdCl₂. These latter species were not detectable by XRD at all.

Palladium chloride can exist in at least

TABLE 1

Infrared and Raman Band Positions for PdCl$_2$ and Compounds Derived from PdCl$_2$

Compound	Spec.[a]	Band positions (cm^{-1})	Ref.
PdCl$_2(\alpha)$	R	274(vs), 313(vs), 370(w)	This work
PdCl$_2(\beta)$	R	147(s), 206(w), 278(vs), 295 (sh), 335(s)	This work
PdCl$_2$	IR	174(mw), 287(vw), 297(vw), 340(vs), 348(sh)	(26)
PdCl$_4^{2-}$	IR	151, 161, 321	(27)
	R	164, 275, 303	
PdCl$_6^{2-}$	R	164(m), 292(m), 317(s)	(28)
Pd^{II}(NH$_3$)$_2$Cl$_2$	R	295	(29)
Pd^{IV}(NH$_3$)$_2$Cl$_2$	R	295, 317	(30)
Pd^{II}Pd^{IV}(NH$_3$)$_4$Cl$_4$	R	295(w), 303(w), 316(s)	(30)
PdCl$_2$: Al$_2$Cl$_6$	R	84.5(vs), 176(m), 298(s)	(31)

[a] IR, Infrared spectroscopy; R, Raman spectroscopy.

three crystalline forms (32–34). The best known is the α form which consists of infinite chains of coplanar PdCl$_{4/2}$ units. The β form is hexameric Pd$_6$Cl$_{12}$ with octahedral clusters of Pd atoms. No structural information is yet available about the third polymorph. Differential thermal analysis of PdCl$_2$ prepared at low temperature indicates that endothermal transitions occur at 673 and 773 K (32). The X-ray diffraction pattern of PdCl$_2$ in the intermediate temperature range is clearly identified as the α form. Since the β-form is known to convert to the α-form at elevated temperature (33), it is presumed that below 673 K, PdCl$_2$ is in the β form. Taking these facts into account, we propose that spectrum 5a can be attributed to the β form of PdCl$_2$ and that spectrum 5b, taken after heating PdCl$_2$ to 673 K, is that of the α form. Thus, it appears that laser Raman spectroscopy can be used to follow the β to α transformation.

The spectrum of PdCl$_2$ supported on SiO$_2$ is illustrated in Fig. 6 (spectrum a). The bands at 283, 313, and 347 cm^{-1} strongly resemble the features observed in spectra 5a and 5b, which have been attributed to the β and α forms of PdCl$_2$, respectively. The bands appearing at 76, 105, and 130 cm^{-1} in spectrum 6a were not present in the spectra of either form of PdCl$_2$. No definite

assignment can be given to these features, but their low frequencies suggest that they may be due to lattice vibrations. It is interesting to note that three bands were observed in the Pd 3d$_{5/2}$ portion of the XPS spectrum of silica-supported PdCl$_2$ (5). These features occur at 337.9, 337.0, and 335.9 eV and have been attributed to PdCl$_4^{2-}$, PdCl$_2$(H$_2$O)$_2$, and Pd(H$_2$O)$_4^{2+}$, respectively. The extent to which the species containing water might contribute to the ap-
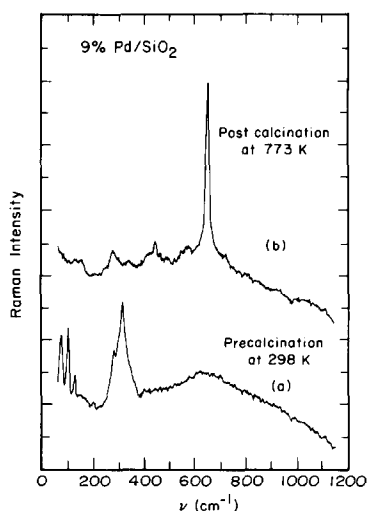

FIG. 6. Raman spectra of SiO$_2$ supported PdCl$_2$ (as H$_2$PdCl$_4$): (a) at 298 K; (b) following calcination in air at 773 K for 2.5 hr.
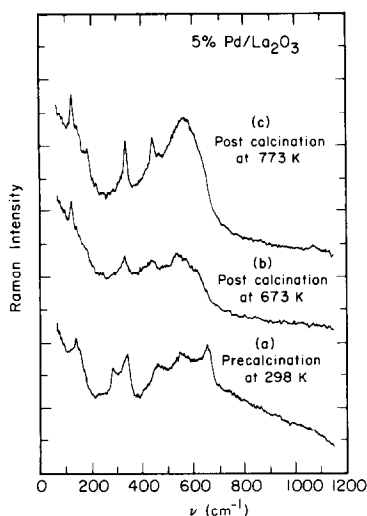
FIG. 7. *In situ* Raman spectra of La(OH)$_3$ ion exchanged with H$_2$PdCl$_4$: (a) at 298 K; (b) following calcination in air at 673 K for 30 min; (c) following calcination in air at 773 K for 3 hr.

pearance of Raman bands below 140 cm^{-1} is unknown.

Spectrum 6b was obtained following calcination of the silica-supported PdCl$_2$ at 773 K for 2.5 hr. The very strong resemblance of this spectrum to spectrum 5c indicates that during calcination a majority of the PdCl$_2$ was converted to PdO. The XRD pattern of this sample shows that the palladium was not only oxidized but also agglomerated to bulk-like oxide. This oxidation was confirmed also by XPS (5). The Pd 3d$_{5/2}$ binding energy of the calcined sample was equal to 336.3 eV, in good agreement with what was expected for PdO.

The Raman spectrum of hydrated La$_2$O$_3$ ion exchanged with H$_2$PdCl$_4$ is shown in Fig. 7 (spectrum a). The bands appearing at 139, 224, 339, and 459 closely resemble those observed for La(OH)$_3$ seen in spectrum 3b and, hence, are attributed to the support. The remaining two bands at 651 and 546 cm^{-1} in spectrum 7a cannot be assigned definitively. The band at 651 cm^{-1} might be attributed to PdO on the basis of a comparison with spectrum 5c, but this seems unreasonable since the band at 651 cm^{-1} was observed already at room temper-

ature and prior to calcination. An alternative explanation is that both the 651 and 546 cm^{-1} bands are due to some product formed upon the reaction of H$_2$PdCl$_4$ with La(OH)$_3$. This interpretation agrees with the observation of a single peak at 336.9 eV in the Pd XPS spectrum, which has been assigned to a palladium aquochloride species (5).

The spectrum taken after *in situ* calcination in dry air at 673 K (spectrum 7b) was significantly different from that seen originally. The band at 139 cm^{-1} was replaced by one at 121 cm^{-1}, the band at 285 cm^{-1} disappeared, and the band at 459 cm^{-1} shifted to about 440 cm^{-1}. It was also observed that following calcination, the band at 651 was attenuated greatly relative to the band at 540 cm^{-1}. Raising the calcination temperature to 773 K produced yet further changes in the spectrum (spectrum 7c). The bands at 124, 333, and 440 were more intense than the corresponding features in spectrum 7b, and a new feature was now evident at 179 cm^{-1}. It was also seen that the broad band at 540 cm^{-1} increased in intensity and shifted to 563 cm^{-1}.

Comparison of spectrum 7c with spectrum 3b indicates that the presence of Pd on the support influences the structure of the LaO$_3$ support following calcination. Thus, the features appearing at 105, 190, 316, and 407 cm^{-1} when the support was calcined appeared at 124, 179, 333, and 440 cm^{-1}, when Pd was present. It is also evident from a comparison of the spectra for calcined Pd/SiO$_2$ and Pd/La$_2$O$_3$, that in the latter case Pd was not converted to PdO. The broad band at 563 cm^{-1}, seen in spectrum 7c, is quite different from the narrow, intense line at 651 cm^{-1} assigned to PdO, seen in spectrum 6c or spectrum 5c. It is also significant to note that the XRD pattern of calcined Pd/La$_2$O$_3$ showed no evidence of PdO, La$_2$O$_3$, or La(OH)$_3$. Surprisingly, the XRD pattern could be best represented by crystalline LaOCl. This interpretation is supported by the correspondence of the Raman lines appearing at 124, 179, 333, and 440 cm^{-1} with those reported for pure

LaOCl at 125, 188, 335, and 440 (*35*). Thus, it appears that part of the chlorine associated originally with PdCl$_2$ may react with La(OH)$_3$ during calcination to form LaOCl. The form in which Pd is present cannot be clearly defined. However, it is certain that Pd is present in an oxidized state, since XPS spectra of calcined Pd/La$_2$O$_3$ (*5*) show that the Pd 3d$_{5/2}$ binding energy is 336.2 eV, identical to that for PdO. Conceivably, the Pd atoms are contained in a mixed metal oxide involving both Pd and La. Evidence for the formation of materials such as La$_2$PdO$_4$ and La$_4$PdO$_7$ has been presented in the literature (*36*).

As noted in the Introduction, recently reported studies by Fleisch *et al.* (*5*) and Hicks *et al.* (*4, 6*) suggest that the surface of Pd crystallites supported on La$_2$O$_3$ are covered by thin patches of LaO following reduction. To determine whether the structure of these patches could be distinguished from that of the support, Raman spectra were recorded during the *in situ* reduction of the calcined Pd/La$_2$O$_3$ sample. Upon heating in a 12% H$_2$ in Ar mixture at 423 K, the color of the sample changed from a medium intensity grey to dark grey. The broad band at 563 cm^{-1} disappeared completely from the spectrum, but bands at 124, 179, 333, and 435 cm^{-1} associated with the support could still be seen. Elevation of the temperature to 523 K caused a further darkening in the color of the sample and an attenuation in the intensity of the bands attributed to the support; however, no new features were observed. Subsequent *in situ* exposure of the sample to dry air to 523 and 623 K resulted in the reappearance of the broad band at 563 cm^{-1} and an intensification of the bands for the support.

The results obtained during the *in situ* reduction of calcined Pd/La$_2$O$_3$ further support the assignment of the feature at 563 cm^{-1} to a form of oxidized Pd. The deepening in the sample color with extent of reduction and the loss of intensity in the support bands were both indicative of an increase in the optical absorbance of the sample as re-

duction proceeded. As a consequence, Raman scattering occurred from a progressively thinner layer located near the front surface of the pressed disc. When the sample was reoxidized, the layer sampled became thicker due to a decrease in the absorbance of the sample.

The present investigation demonstrates that the chemical species involved in the genesis of supported Pd from PdCl$_2$ differ significantly depending on whether SiO$_2$ or La$_2$O$_3$ is used as the support. In particular is seen that following calcination Pd exists as well defined PdO crystallites on SiO$_2$ but appears to form a mixed meal oxide involving both Pd and La when the support is La$_2$O$_3$. Unfortunately, though, Raman spectroscopy does not permit characterization of the reduced metal catalyst. It is possible to infer, though, that the difference in the structure of the two catalysts in the calcined state are responsible, in some fashion, for the observed differences in the Pd 3d$_{5/2}$ binding energies of reduced Pd/SiO$_2$ and Pd/La$_2$O$_3$ discussed by Fleisch *et al.* (*5*).

CONCLUSIONS

Laser Raman spectroscopy provides useful information regarding the chemistry occurring during the preparation of silica and lanthanum oxide-supported Pd catalysts. No spectral features are observed between 50 and 1200 cm^{-1} for silica. Well-defined bands are observed, though, for the lanthanum oxide support. The spectrum of this material depends on its degree of hydration. Fully hydrated lanthanum oxide is present as La(OH)$_3$. Heating in dry air leads to a progressive dehydration of La(OH)$_3$ back to La$_2$O$_3$. Evidence for intermediate structures such as [La(OH)$_2$O]$_2$O and La(OH) has been obtained. Several transformations were observed during the calcination of unsupported PdCl$_2$. Around 673 K, β-PdCl$_2$ is observed to convert to α-PdCl$_2$. At higher temperatures PdCl$_2$ is converted fully to PdO. The spectrum of silica supported PdCl$_2$ (as H$_2$PdCl$_4$) suggests that

PdCl$_2$ is present in both its α and β forms. Upon calcination at 773 K, the PdCl$_2$ is again converted to PdO. The spectrum of fully hydrated lanthanum oxide [La(OH)$_3$] ion exchanged with H$_2$PdCl$_4$ is distinctly different from that of H$_2$PdCl$_4$ supported on silica. The exact form of the Pd cannot be determined from the spectrum, but there is some indication that the metal is in an oxidized state. Calcination of the sample produces a broad feature which is thought to be due to a mixed metal oxide of La and Pd. This feature is eliminated completely when the calcined sample is reduced.

REFERENCES

1. Ichikawa, M., *Shokubai* 21, 253 (1979).
2. Ryndin, Yu. A., Hicks, R. F., Bell, A. T., and Yermakov, Yu. I., *J. Catal.* 70, 287 (1981).
3. Poels, E. K., van Broekhoeven, E. H., van Barneveld, W. A. A., and Ponec, V., *React. Kinet. Catal. Lett.* 18, 223 (1981).
4. Hicks, R. F., Bell, A. T., and Fleisch, T. H., *Appl. Surface Sci.,* in press.
5. Fleisch, T. H., Hicks, R. F., and Bell, A. T., *J. Catal.* 87, 398 (1984).
6. Hicks, R. F., Yen, Q. J., and Bell, A. T., *J. Catal.,* in press.
7. Aben, P. C., *J. Catal.* 10, 224 (1968).
8. Boldish, S. I., and White, W. B., *Spectrachim. Acta* 35, 1235 (1979).
9. Zarembowitch, J., Gouteron, J., and Lejus, A. M., *Phys. Status Solidi B* 94, 249 (1979).
10. Gopinath, C. R., and Brown, I. D., *J. Raman Spec.* 12, 278 (1982).
11. Swanson, B. I., Machell, C., Beall, G. W., and Milligan, W. O., *J. Inorg. Nucl. Chem.* 40, 694 (1978).
12. Hutting, G. F., *Uspekhi Khim.* 4, 399 (1935).
13. Hutting, G. F., and Kantor, K., *Z. Anorg. Chem.* 202, 421 (1938).
14. Shafer, M. W., and Ray, R., *J. Amer. Ceram. Soc.* 42, 563 (1959).
15. Blum, S. H., and Maquire, E. A., *Amer. Ceram. Bull.* 39, 320 (1960).
16. Klevtsov, P. V., and Sheina, L. P., *Izv. Akad. Nauk SSR, Ser. Neorg. Materialy* 1, 912, 2219 (1965).
17. Zubova, N. V., Makarova, V. M., Nikol'skii, V. D., Petrov, P. N., Teterin, E. G., and Chevotarev, N. T., *Russ. J. Inorg. Chem.* 13, 7 (1968).
18. Rybakova, B. N., Moskvicheva, A. F., and Beregovaya, G. D., *Russ. J. Inorg. Chem.* 1, 1531 (1969).
19. Siegmann, H. C., Schlapbach, L., and Brundle, C. R., *Phys. Rev. Lett.* 40, 972 (1978).
20. Schlapbach, L., Seiler, A., Siegmann, H. C., Waldkirch, T. V., Zürcher, P., and Brundle, C. R., *Int. J. Hydrogen Energy* 4, 21 (1979).
21. Petru, F., Kutek, F., and Satova, J., *Collec. Czech. Chem. Comm.* 31, 4459 (1966).
22. Kletsov, P. V., Kletsova, R. F., and Sheina, L. P., *Zhur. Struk. Khim.* 8, 268 (1967).
23. Goldsmith, J. A., and Ross, S. D., *Spectrachim. Acta* 23A, 1909 (1967).
24. Taravel, B., Fromage, F., Delorme, P., and Lorenzelli, V., *J. Chim. Phys. Physicochem. Biol.* 68, 715 (1971).
25. Rosynek, M. P., and Magnuson, D. T., *J. Catal.* 48, 417 (1977).
26. Adams, D. M., Goldstein, M., and Mooney, E. F., *Trans. Faraday Soc.* 59, 2228 (1963).
27. Bosworth, Y. M., and Clark, R. J. H., *Inorg. Chem.* 14, 170 (1975).
28. Woodward, L. A., and Creighton, J. A., *Spectrachim. Acta* 17, 594 (1961).
29. Perry, C. H., Athans, D. P., Young, E. F., Durig, J. R., and Mitchell, B. R., *Spec. Acta* 23A, 1137 (1967).
30. Clark, R. J. H., and Trumble, W. R., *Inorg. Chem.* 15, 1030 (1976).
31. Papatheodorou, G. M., and Capote, M. A., *J. Chem. Phys.* 69, 2067 (1978).
32. Fishman, E., and Sugmagne, P., *J. Phys. Chem.* 69, 3669 (1965).
33. Schäfer, H., Wiese, U., Rinke, K., and Brendel, K., *Angew. Chem. Int. Ed.* 6, 253 (1967).
34. Canterford, J. H., and Colton, R., "Halides of the Second and Third Row Transition Metals." Wiley, New York, 1968.
35. Hase, Y., Dunstan, L. P. O., and Temperini, M. L. A., *Spectrochim. Acta* 37A, 597 (1981).
36. Kakhan, B. G., Lazarev, V. B., and Shaplygin, I. S., *Term. Anal. Tezisy. Dokl. Vses. Sovesch. 7th 1979 (USSR)* 1, 234 (1979); CA 93-29975q.